

Intention-Aware Motion Planning Using Learning Based Human Motion Prediction

Jae Sung Park and Chonhyon Park and Dinesh Manocha
<http://gamma.cs.unc.edu/SafeMP> (video included)

Abstract—We present a motion planning algorithm to compute collision-free and smooth trajectories for robots cooperating with humans in a shared workspace. Our approach uses offline learning of human actions and their temporal coherence to predict the human actions at runtime. This data is used by an intention-aware motion planning algorithm that is used to compute a reliable trajectory based on these predicted actions. We highlight the performance of our planning algorithm in complex simulated scenarios and real world scenarios with 7-DOF robot arms operating in a workspace with a human performing complex tasks. We demonstrate the benefits of our intention-aware planner in terms of computing safe trajectories.

I. INTRODUCTION

Motion planning algorithms are used to compute collision-free paths for robots among obstacles. Most of the techniques have been designed for static environments with known obstacle positions. As robots are increasingly used in workspaces with moving or unknown obstacles, it is important to develop reliable planning algorithms that can handle environmental uncertainty and the dynamic motions. In particular, we address the problem of planning safe and reliable motions for a robot that is working in environments with humans. As the humans move, it is important for the robots to predict the human actions and motions from sensor data and to compute appropriate trajectories.

In order to compute reliable motion trajectories in such shared environments, it is important to gather the state of the humans as well as predict their motions. There is considerable work on realtime tracking of human motion in computer vision and related areas [1], [2]. However, the current state of the art in collecting such motion data results in many challenges. First of all, there are errors in the data due to the sensors (e.g., point-cloud sensors) or poor sampling. Secondly, human motion can be sudden or abrupt and this can result in various uncertainties in the environment representation. One way to overcome some of these problems is to use predictive or estimation techniques for human motion or actions, such as using various filters like Kalman filters or particle filters [3], [4]. Most of these prediction algorithms use a motion model that can predict future motion based on the prior positions of human body parts or joints, and corrects the error between the estimates and actual measurements. In practice, these approaches work well when there is sufficient information about prior motion

Jae Sung Park and Chonhyon Park and Dinesh Manocha are with the Department of Computer Science, University of North Carolina at Chapel Hill. E-mail: {jaesungp, chpark, dm}@cs.unc.edu.

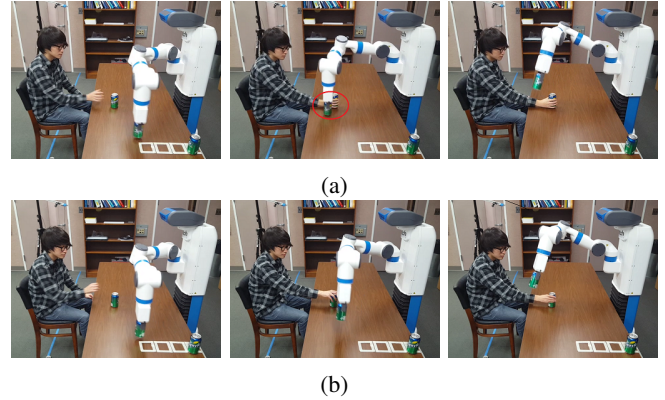


Fig. 1: A 7-DOF Fetch robot is moving its arm near a human, avoiding collisions. (a) While the robot is moving, the human tries to move his arm to block the robot's path. The robot arm trajectory is planned without human motion prediction, making collisions and a jerky trajectory, shown in the red circle. This is because the speed of human arm is too fast for robot to avoid collision. (b) The trajectory is planned with human motion prediction, avoid collisions and results in smoother trajectories. The robot's trajectory detours in advance to avoid future possible collisions.

that can be accurately modeled by the underlying motion model. However, these estimates can be inaccurate where there is not sufficient data about human motions, or the prior motions of humans can't be accurately captured by the underlying motion models.

In some scenarios, it is possible to infer high-level human intent using additional information, and thereby to perform a better prediction of future human motions [5], [6]. These techniques are used to predict the pedestrian positions for autonomous vehicles based on environmental information, such as the location of crosswalks or traffic light signals. However, these techniques are limited to the 2D trajectories of the pedestrians on the ground.

Main Results: In this paper, we present a novel motion planning algorithm to compute safe and collision-free trajectories for robots operating in workspaces involved in human-robot cooperating scenarios, where the robot and a human perform manipulation tasks simultaneously. In our case, it is important to develop intention-aware techniques that can predict the actions of humans that correspond to high-DOF models. Furthermore, we need to incorporate these human intentions into a motion planning framework that can avoid collisions

with the humans and other obstacles in the scene, and still generate smooth trajectories that also satisfy other kinematic and dynamic constraints. We use offline training to generate a database of human actions. At runtime, our approach uses the trained human actions and their temporal coherence to predict the future motion from the captured point-cloud data. We use a realtime algorithm to perform probabilistic collision detection between the point cloud representation of a human and the robot, as the robot computes the trajectory for the high level task. These predicted human actions and probabilistic cost functions are integrated into a trajectory optimization algorithm that tends to compute smooth paths as well as satisfy other kinematics and dynamics constraints. We highlight the performance of our planner in a simulator with a 7-DOF KUKA arm operating and in a real world setting with a 7-DOF Fetch robot arm in a workspace with a moving human and performing cooperative tasks. We demonstrate the benefits of our intention-aware planner in terms of avoiding collisions with the humans. The prediction scheme can improve the performance in terms of collision avoidance and smoother trajectories. Our approach can be used in scenarios where the robot needs to treat each human as a dynamic obstacle and avoid collisions with it. Or it can be used in human-robot cooperating scenarios, where they jointly perform some tasks.

The rest of paper is organized as follows. In Section II, we give a brief survey of prior work. Section III presents an overview of our human intention-aware motion planning algorithm. Offline learning and runtime prediction of human motions are described in Section IV, and these are combined with our optimization based motion planning algorithm in Section V. Finally, we demonstrate the performance of our planning framework for a 7-DOF robot in Section VI.

II. RELATED WORKS

In this section, we provide a brief overview of the relevant prior work on human motion prediction, task planning for human-robot collaborations, and motion planning in environments shared with humans.

A. Intention-Aware Motion Planning and Human Motion Prediction

Intention-Aware Motion Planning (IAMP) denotes a motion planning framework where the uncertainty of human intention is taken into account [5]. The goal position and the trajectory of moving pedestrians can be considered as human intention and used so that a moving robot can avoid pedestrians [7].

In terms of robot navigation among obstacles and pedestrians, accurate predictions of humans or other robot positions are possible based on crowd motion models [8], [9] or integration of motion models with online learning techniques [10], [11]. However, most of these methods are limited to navigation on 2D planes.

Predicting the human actions or the high degrees-of-freedom (DOF) human motions has several challenges. Estimated human poses from recorded videos or realtime sensor

data tend to be inaccurate or imperfect due to occlusions or limited sensor ranges. Furthermore, the whole-body motions and their complex dynamics with many high DOF make it difficult to represent them with accurate motion models.

There has been a considerable literature on recognizing human actions [12]. Machine learning-based algorithms using Gaussian Process Latent Variable Models (GP-LVM) [13], [14] or Recurrent neural network (RNN) [15] have been proposed to compute accurate human dynamics models. Recent approaches use the learning of human intentions along with additional information, such as temporal relations between the actions [16], [17] or object affordances [18], which result in improved accuracy in terms of predicting the human actions.

B. Robot Task Planning for Human-Robot Collaboration

In human-robot collaborative scenarios, robot task planning algorithms have been developed for the efficient distribution of subtasks. One of their main goal is reducing the completion time of the overall task by interleaving subtasks of robot with subtasks of humans with well designed task plans. In order to compute the best action policy for a robot, Markov Decision Processes (MDP) have been widely used [19]. Nikolaidis et al. [16] use MDP models based on mental model convergence of human and robots. Koppula and Saxena [20] use Q-learning to train MDP models where the graph model has the transitions corresponding to the human action and robot action pairs. Our MDP models extend these approaches, but also take into account the issue of avoiding collisions between the human and the robot.

C. Motion Planning in Environments shared with Humans

Prior work on motion planning in the context of human-robot interaction has focused on computing robot motions that satisfy cognitive constraints such as social acceptability [21] or being legible to humans [22].

In human-robot collaboration scenarios where both the human and the robot perform manipulation tasks in a shared environment, it is important to compute robot motions that avoid collisions with the humans for safety reasons. Dynamic window approach [23] (which searches the optimal velocity in a short time interval) and realtime replanning [24], [25] (which interleaves planning with execution) are widely used approaches for planning in such dynamic environments. As there are uncertainties in the prediction model and in the sensors for human motion, the future pose is typically represented as the *Belief* state, which corresponds to the probability distribution over all possible human states. Mainprice and Berenson [26] explicitly construct an occupied workspace voxel map from the predicted Belief states of humans in the shared environment and avoid collisions.

III. OVERVIEW

In this section, we first introduce the notation and terminology used in the paper and give an overview of our motion planning algorithms.

A. Notation and Assumptions for Learning and Prediction

As we need to learn about human actions and short-term motions, a large training dataset of human motions is needed. We collect N demonstrations of how human joints typically move while performing some tasks and in which order subtasks are performed. Each demonstration is represented using $T^{(i)}$ frame of human joint motion, where the superscript (i) represents the demonstration index. The motion training dataset is represented as following:

- ξ is a matrix of tracked human joint motions. $\xi^{(i)}$ has $T^{(i)}$ columns, where a column vector represents the different human joint positions during each frame.
- F is a feature vector matrix. $F^{(i)}$ has $T^{(i)}$ columns and is computed from $\xi^{(i)}$.
- \mathbf{a}^h is a human action (or subtask) sequence vector that represents the action labels over different frames. For each frame, the action is categorized into one of the m^h discrete action labels, where the action label set is $A^h = \{a_1^h, \dots, a_{m^h}^h\}$.
- $L = \{(\xi^{(i)}, F^{(i)}, \mathbf{a}^{h,(i)})\}_{i=1}^N$ is the motion database used for training. It consists of human joint motions, feature descriptors and the action labels at each frame.

During runtime, MDP-based human action inference is used in our task planner. The MDP model is defined as a tuple (P, A^r, T) :

- $A^r = \{a_1^r, \dots, a_{m^r}^r\}$ is a robot action (or subtask) set of m^r discrete action labels.
- $P = \mathcal{P}(A^r \cup A^h)$, a power set of union of A^r and A^h , is the set of states in MDP. We refer to the state \mathbf{p} as a *progress state* because each state represents which human and robot actions have been performed so far. We assume that the sequence of future actions for completing the entire task depends on the list of actions completed. \mathbf{p} has $m^h + m^r$ binary elements, which represent corresponding human or robot actions have been completed ($\mathbf{p}_j = 1$) or not ($\mathbf{p}_j = 0$).
- $T : P \times A^r \rightarrow \Pi(P)$ is a transition function. When a robot performs an action a^r in a state \mathbf{p} , $T(\mathbf{p}, a^r)$ is a probability distribution over the progress state set P . The probability of being state \mathbf{p}' after taking an action a^r from state \mathbf{p} is denoted as $T(\mathbf{p}, a^r, \mathbf{p}')$.
- $\pi : P \rightarrow A^r$ is the action policy of a robot. $\pi(\mathbf{p})$ denotes the best robot action that can be taken at state \mathbf{p} , which results in maximal performance.

We use the Q-learning [27] to determine the best action policy during a given state, which rewards the values that are induced from the result of the execution.

B. Notation for Robot

We denote a single configuration of the robot as a vector \mathbf{q} that consists of joint-angles. The n -dimensional space of configuration \mathbf{q} is the configuration space \mathcal{C} . We represent each link of the robot as R_i . The finite set of bounding spheres for link R_i is $\{B_{i1}, B_{i2}, \dots\}$, and is used as a bounding volume of the link, i.e., $R_i \subset \cup_j B_{ij}$. The links and bounding spheres at a configuration \mathbf{q} are denoted as $R_i(\mathbf{q})$

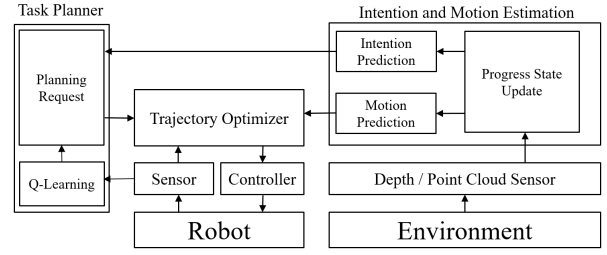


Fig. 2: **Overview of our Intention-Aware Planner:** Our approach consists of three main components: task planner, trajectory optimization, and intention and motion estimation. They are combined at runtime to perform realtime safe motion planning.

and $B_{ij}(\mathbf{q})$, respectively. In our benchmarks, where the robot arms are used, these bounding spheres are automatically generated using the medial axis of robot links. We also generate the bounding spheres $\{C_1, C_2, \dots\}$ for humans and other obstacles.

For a planning task with start and goal configurations \mathbf{q}_s and \mathbf{q}_g , the robot's trajectory is represented by a matrix \mathbf{Q} ,

$$\mathbf{Q} = \begin{bmatrix} \mathbf{q}_s & \mathbf{q}_1 & \dots & \mathbf{q}_{n-1} & \mathbf{q}_g \\ t_0 & t_1 & \dots & t_{n-1} & t_n \end{bmatrix},$$

where robot trajectory passes through the $n + 1$ waypoints. We denote the i -th waypoint of \mathbf{Q} as $\mathbf{x}_i = [\mathbf{q}_i^T \ t_i]$.

C. Motion Planning Algorithm

The main goals of our motion planner are: (1) planning high-level tasks for a robot by anticipating the most likely next human action and (2) computing a robot trajectory that reduces the probability of collision between the robot and the human or other obstacles, by using motion prediction.

At the high-level task planning step, we use MDP, which is used to compute the best action policies for each state. The state of an MDP graph denotes the progress of the whole task. The best action policies are determined through reinforcement learning with Q-learning. Then, the best action policies are updated within the same state. The probability of choosing the action increases or decreases according to the reward function. Our reward computation function is affected by the prediction of intention and the delay caused by predictive collision avoidance.

We also estimate the short-term future motion from learned information. From the joint position information, motion features are extracted based on human poses and surrounding objects related to human-robot interaction tasks, such as joint positions of humans, relative positions from a hand to other objects, etc. We use a Dynamic Time Warping (DTW) [28] kernel function for incorporating the temporal information. Given the human motions database of each action type, we train future motions using Sparse Pseudo-input Gaussian Process (SPGP) [29]. The final future motion is computed as the weighted sum over different action types weighed by the probability of each action type that could be performed next.

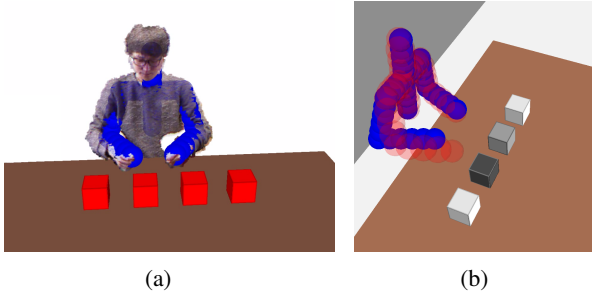


Fig. 3: **Motion uncertainty and prediction:** (a) A point cloud and the tracked human (blue spheres). The joint positions are used as feature vectors. (b) Prediction of next human action and future human motion, where 4 locations are colored according to their probability of next human action from white (0%) to black (100%). Prediction of future motion after 1 second (red spheres) from current motion (blue spheres) is shown as performing the action: *move right hand to the second position* which has the highest probability associated with it.

After deciding which robot task will be performed, the robot motion trajectory is then computed that tends to avoid collisions with humans. An optimization-based motion planner (ITOMP) [25] is used to compute a locally optimal solution that minimizes the objective function subject to many types of constraints such as robot related constraints (e.g., kinematic constraint), human motion related constraints (e.g., collision free constraint), etc. Because future human motion is uncertain, we can only estimate the probability distribution of the possible future motions. Therefore, we perform probabilistic collision checking to reduce the collision probability in future motions. We also continuously track the human pose and update the predicted future motion to re-plan safe robot motions. Our approach uses the notion of realtime probabilistic collision detection [30] between the robot and the point-cloud data corresponding to human obstacles, to compute reactive costs and integrate them with our optimization-based planner.

IV. HUMAN ACTION PREDICTION

In this section, we describe our human action prediction algorithm, which consists of offline learning and online inference of actions.

A. Learning of Human Actions and Temporal Coherence

We collect N demonstrations of the whole task to form a motion database L . The 3D joint positions are tracked using OpenNI library [31], and their coordinates are concatenated to form a column vector $\xi^{(i)}$.

In order to learn the temporal coherence between the actions, we deal with only the human action sequences $\{\mathbf{a}^{h,(i)}\}_{i=1}^N$. Based on the progress state representation, for any time frame s , the prefix sequence of $\mathbf{a}^{h,(i)}$ of length s yields a progress state $\mathbf{p}_s^{(i)}$ and the current action $c_s^{h,(i)} = \mathbf{a}_s^{h,(i)}$. The next action label $n_s^{h,(i)}$ performed after frame s can also be computed, at which the action label differs at the first time while searching in the increasing order from

frame $s+1$. Then, for all possible pairs of demonstrations and frame index (i, s) , the tuples $(\mathbf{p}_s^{(i)}, c_s^{h,(i)}, n_s^{h,(i)})$ are collected to compute histograms $h(n^h; \mathbf{p}, c^h)$, which counts the next action labels at each pair (\mathbf{p}, c^h) that have appeared at least once. We use the normalized histograms to estimate the next future action for the given \mathbf{p} and c^h . i.e.,

$$p(n^h = a_j^h | \mathbf{p}, c^h) = \frac{h(a_j^h; \mathbf{p}, c^h)}{\sum_{k=1}^m h(a_k^h; \mathbf{p}, c^h)}. \quad (1)$$

In the worst case, there are at most $O(2^m)$ progress states since there are m binary values per action. However, in practice, only $O(N \cdot m)$ progress states are generated. It is because the number of unique progress states are less than m , and the subtask order dependency may allow only a few possible topological orders.

In order to train the human motion, the motion sequence $\xi^{(i)}$ and the feature sequence $F^{(i)}$ are learned, as well as the action sequences $\mathbf{a}^{(i)}$. Because we are interested in short-term human motion prediction for collision avoidance, we train the learning module from multiple short periods of motion. Let n_p be the number of previous consecutive frames and n_f be the number of future consecutive frames to look up. n_f and n_p are decided so that the length of motion is short-term motion (e.g. about 1 second). At the time frame s , where $n_p \leq s \leq T^{(i)} - n_f$, the columns of feature matrix $F^{(i)}$ from column index $s - n_p + 1$ to s are denoted as $F_{prev,s}^{(i)}$. Similarly, the columns of motion matrix from index $s + 1$ to $s + n_f$ are denoted as $\xi_{next,s}^{(i)}$.

Tuples $(F_{prev,s}^{(i)}, \mathbf{p}_s^{(i)}, c_s^{h,(i)}, \xi_{next,s}^{(i)})$ for all possible pairs of (i, s) are collected as the training input. They are partitioned into groups having the same progress state \mathbf{p} . For each progress state \mathbf{p} and current action c^h , the set of short-term motions are regressed using SPGP with the DTW kernel function [28], considering $\{F_{prev}\}$ as input and $\{\xi_{next}\}$ as multiple channeled outputs. We use SPGP, a variant of Gaussian Processes, because it significantly reduces the running time for training and inference by choosing M pseudo-inputs from a large number of an original human motion inputs. The final learned probability distribution is

$$p(\xi_{next,c} | F_{prev}, \mathbf{p}, c^h) = \prod_{c: \text{channels}} p(\xi_{next,c} | F_{prev}, \mathbf{p}, c^h), \quad (2)$$

where $\mathcal{GP}(\cdot, \cdot)$ represents trained SPGPs, c is an output channel (i.e., an element of matrix ξ_{next}), and m_c and K_c are the learned mean and covariance functions of the output channel c , respectively.

The current action label $c_s^{h,(i)}$ should be learned to estimate the current action. We train $c_s^{h,(i)}$ using Tuples $(F_{prev,s}^{(i)}, \mathbf{p}_s^{(i)}, c_s^{h,(i)})$. For each state \mathbf{p} , we use Import Vector Machine (IVM) classifiers to compute the probability distribution:

$$p(c^h = a_j^h | F_{prev}, \mathbf{p}) = \frac{\exp(f_j(F_{prev}))}{\sum_{a_k^h} \exp(f_k(F_{prev}))}, \quad (3)$$

where $f_j(\cdot)$ is the learned predictive function [32] of IVM.

B. Runtime Human Intention and Motion Inference

Based on the learned human actions, at runtime we infer the next most likely short-term human motion and human subtask for the purpose of collision avoidance and task planning, respectively. The short-term future motion prediction is used for the collision avoidance during the motion planning. The probability of future motion is given as:

$$p(\xi_{future}|F, \mathbf{p}) = \sum_{c^h \in A^h} p(\xi_{future}, c^h|F, \mathbf{p}).$$

By applying the Bayes theorem, we get

$$p(\xi_{future}|F, \mathbf{p}) = \sum_{c^h \in A^h} p(c^h|F, \mathbf{p})p(\xi_{future}|F, \mathbf{p}, c^h). \quad (4)$$

The first term $p(c^h|F, \mathbf{p})$ is inferred through the IVM classifier in (3). To infer the second term, the nearest cluster from feature F with respect to (\mathbf{p}, c^h) is computed and identified with the index k . Then we use the probability distribution in (2) for each output channel.

We use Q-learning for training the best robot action policy π in our MDP-based task planner. We first define the function $Q : P \times A^r \rightarrow \mathbb{R}$, which is iteratively trained with the motion planning executions. Q is updated as

$$Q_{t+1}(\mathbf{p}_t, a_t^r) = (1 - \alpha_t)Q_t(\mathbf{p}_t, a_t^r) + \alpha_t(R_{t+1} + \gamma \max_{a^r} Q_t(\mathbf{p}_{t+1}, a^r)),$$

where the subscripts t and $t + 1$ are the iteration indexes, R_{t+1} is the reward function after taking action a_t^r at state \mathbf{p}_t , and α_t is the learning rate. A reward value R_{t+1} is determined by several factors:

- Preparation for next human action: the reward gets higher when the robot runs an action before a human action which can be benefited by the robot's action. We define this reward as $R_{prep}(\mathbf{p}_t, a_t^r)$. Because the next human subtask depends on the uncertain human decision, we predict the likelihood of the next subtask from the learned actions in (1) and use it for the reward computation. The reward value is given as

$$R_{prep}(\mathbf{p}_t, a_t^r) = \sum_{a^h \in A^h} p(n^h = a^h|\mathbf{p}_t)H(a^h, a_t^r), \quad (5)$$

where $H(a^h, a^r)$ is a prior knowledge of reward, representing the amount of how much the robot helped the human by performing the robot action a^r before the human action a^h . If the robot action a^r has no relationship with a^h , the H value is zero. If the robot helped, the H value is positive, otherwise negative.

- Execution delay: There may be a delay in the robot motion's execution due to the collision avoidance with the human. To avoid collisions, the robot may deviate around the human and make it without delay. In this case the reward function is not affected, i.e. $R_{delay,t} = 0$. However, there are cases that the robot must wait until the human moves to another pose because the human can block the robot's path, which causes delay d . We

penalize the amount of delay to the reward function, i.e. $R_{delay,t} = -d$. Note that the delay can vary during each iteration due to the human motion uncertainty.

The total reward value is a weighted sum of both factors:

$$R_{t+1} = w_{prep}R_{prep}(\mathbf{p}_t, a_t^r) + w_{delay}R_{delay,t}(\mathbf{p}_t, a_t^r),$$

where w_{prep} and w_{delay} are weights for scaling the two factors. The preparation reward value is predefined for each action pairs. The delay reward is measured during runtime.

V. INTENTION-AWARE ROBOT PLANNING

Our motion planner is based on an optimization formulation, where $n + 1$ waypoints in the space-time domain \mathbf{Q} define a robot motion trajectory to be optimized. Specifically, we use ITOMP [25], which repeatedly refines the trajectory while interleaving the execution and motion planning. We handle three types of constraints: smoothness constraint, static obstacle constraint, and dynamic obstacle constraint. In order to deal with the uncertainty of future human motion, we use probabilistic collision detection between the robot and the predicted future human pose.

Let s be the current waypoint index, meaning that the motion trajectory is executed in the time interval $[t_0, t_s]$, and let m be the replanning time step. A cost function for collisions between the human and the robot is:

$$\sum_{i=s+m}^{s+2m} p \left(\bigcup_{j,k} B_{jk}(\mathbf{q}_i) \cap C_{dyn}(t_i) \neq \emptyset \right) \quad (6)$$

where $C_{dyn}(t)$ are the workspace volumes occupied by dynamic human obstacles at time t . The trajectory being optimized during the time interval $[t_s, t_{s+m}]$ is executed during the next time interval $[t_{s+m}, t_{s+2m}]$. Therefore, the future human poses are considered only in the time interval $[t_{s+m}, t_{s+2m}]$.

The collision probability between the robot and the dynamic obstacle at time frame i in (6) can be computed as a maximum between bounding spheres:

$$\max_{j,k,l} p(B_{jk}(\mathbf{q}_i) \cap C_l(t_i) \neq \emptyset), \quad (7)$$

where $C_l(t_i)$ denotes bounding spheres for a human body at time t_i whose centers are located at line segments between human joints. The future human poses ξ_{future} are predicted in (4) and the bounding sphere locations $C_l(t_i)$ are derived from it. Note that the probabilistic distribution of each element in ξ_{future} is a linear combination of current action proposal $p(c^h|F, \mathbf{p})$ and Gaussians $p(\xi_{future}|F, \mathbf{p}, c^h)$ over all c^h , i.e., (7) can be reformulated as

$$\max_{j,k,l} \sum_{c^h} p(c^h|F, \mathbf{p}) p(B_{jk}(\mathbf{q}_i) \cap C_l(t_i) \neq \emptyset).$$

Let \mathbf{z}_l^1 and \mathbf{z}_l^2 be the probability distribution functions of two adjacent human joints obtained from $\xi_{future}(t_i)$, where the center of $C_l(t_i)$ is located between them by a linear

interpolation $C_l(t_i) = (1-u)\mathbf{z}_l^1 + u\mathbf{z}_l^2$ where $0 \leq u \leq 1$. The joint positions follows Gaussian probability distributions:

$$\mathbf{z}_l^i \sim \mathcal{N}(\mu_l^i, \Sigma_l^i)$$

$$\mathbf{c}_l(t_i) \sim \mathcal{N}((1-u)\mu_l^1 + u\mu_l^2, (1-u)^2\Sigma_l^1 + u^2\Sigma_l^2) \quad (8)$$

$$= \mathcal{N}(\mu_l, \Sigma_l) \quad (9)$$

where $\mathbf{c}_l(t_i)$ is the center of $C_l(t_i)$. Thus, the collision probability between two bounding spheres is bounded by

$$\int_{\mathbb{R}^3} I(\|\mathbf{x} - \mathbf{b}_{jk}(\mathbf{q}_i)\|^2 \leq (r_1 + r_2)^2) f(\mathbf{x}) d\mathbf{x}, \quad (10)$$

where $\mathbf{b}_{jk}(\mathbf{q}_i)$ is the center of bounding sphere $B_{jk}(\mathbf{q}_i)$, r_1 and r_2 are the radius of $B_{jk}(\mathbf{q}_i)$ and $C_l(t_i)$, respectively. The indicator function restricts the integral domain to a solid sphere, and $f(\mathbf{x})$ is the probability density function of $\mathbf{c}_l(t_i)$, in (9). There is no closed form solution for (10), therefore we use the maximum possible value to approximate the probability. We compute \mathbf{x}_{max} at which $f(\mathbf{x})$ is maximized in the sphere domain and multiply it by the volume of sphere, i.e.

$$p(B_{jk}(\mathbf{q}_i) \cap C_l(t_i) \neq \emptyset) \leq V \times f(\mathbf{x}_{max}). \quad (11)$$

Since even \mathbf{x}_{max} does not have a closed form solution, we use the bisection method to find λ with

$$\mathbf{x}_{max} = (\Sigma^{-1} + \lambda I)^{-1}(\Sigma^{-1}\mathbf{p}_{lm} + \lambda\mathbf{o}_{jk}(\mathbf{q}_i)),$$

which is on the surface of sphere, explained in Generalized Tikhonov regularization [33] in detail.

The collision probability, computed in (10), is always positive due to the uncertainty of the future human position, and we compute a trajectory that is probabilistically guaranteed to be collision-free. For a given confidence level δ_{CL} , we compute a trajectory that its probability of collision is upper-bounded by $(1 - \delta_{CL})$. If it is unable to compute a collision-free trajectory, a new waypoint \mathbf{q}_{new} is appended next to the last column of \mathbf{Q} to make the robot wait at the last collision-free pose until it finds a collision-free trajectory. This approach computes a guaranteed collision-free trajectory, but leads to delay, which is fed to the Q-learning algorithm for the MDP task planner. The higher the delay that the collision-free trajectory of a task has, the less likely the task planner selects the task again.

VI. IMPLEMENTATION AND PERFORMANCE

We highlight the performance of our algorithm in a situation where the robot is performing a collaborative task with a human and computing safe trajectories. We use a 7-DOF KUKA-IIWA robot arm in our simulated environment. The human motion is captured by a Kinect sensor operating with a 15Hz frame rate, and only upper body joints are tracked for collision checking. We use the ROS software [34] for robot control and sensor data communication. The number of pseudo-inputs M of SPGPs is set to 100 so that the prediction computation is performed in realtime.

In the simulated benchmark scenario, the human is sitting in front of a desk. In this case, the robot arm helps the human

by delivering objects from one position that is far away from the human to target position closer to the human. The human waits till the robot delivers the object. As different tasks are performed in terms of picking the objects and their delivery to the goal position, the temporal coherence is used to predict the actions. The action set for a human is $A^h = \{Take_0, Take_1, \dots\}$, where $Take_i$ represents an action of taking object i from its current position to the new position. The action set for the robot arm is defined as $A^r = \{Fetch_0, Fetch_1, \dots\}$.

To evaluate the quality of anticipated trajectory of human motion, modified Hausdorff distance (MHD) [35] between the ground-truth human trajectory and the predicted mean trajectory is used. In our experiments, MHD is measured for an actively moving hand joint over 1 second.

We also measured the smoothness of robot's trajectory with and without human motion prediction results. The smoothness is computed as

$$\frac{1}{T} \int_0^T \sum_{i=1}^n \ddot{\mathbf{q}}_i(t)^2, \quad (12)$$

where the two dots indicate acceleration of joint angles.

Table I highlights the performance of our algorithm in three different variations of this scenario: *arrangements of blocks*, *task order* and *confidence level*. Table II shows the performance of our algorithm with a real robot. Our algorithm has been implemented on a PC with 8-core i7-4790 CPU. We used OpenMP to parallelize the computation of future human motion prediction and probabilistic collision checking.

A. Benefits of our Prediction Algorithm

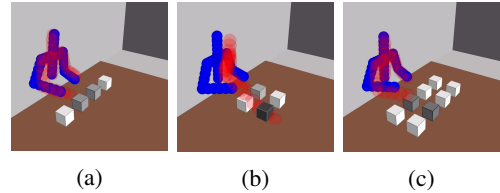


Fig. 4: **Different block arrangements:** Different arrangements in terms of the positions of the blocks, results in different human motions and actions. Our planner computes their intent for safe trajectory planning. The different arrangements are: (a) 1×4 . (b) 2×2 . (c) 2×4 .

In the *Different Arrangements* scenarios, the position and layout of the blocks changes. Fig. 4 shows three different arrangements of the blocks: 1×4 , 2×2 and 2×4 . In the other two cases, where positions are arranged in two rows unlike 1×4 scenario, the human arm blocks a movement from a front position to the back position. As a result, the robot needs to compute its trajectory accordingly.

Depending on the temporal coherence present in the human tasks, the human intention prediction may or may not improve the performance of our the task planner. It is shown in the *Temporal Coherence* scenarios. In the sequential order

Scenarios	Arrangement	Task Order	Confidence Level	Average Prediction Time	MHD	Smoothness	
						No Pred.	Pred.
Different Arrangements	1×4	$(0, 1) \rightarrow (2, 3)$	0.95	52.0 ms	6.7 cm	2.96	1.08
	2×2	$(1, 5) \rightarrow (2, 6)$	0.95	72.4 ms	6.2 cm	5.78	1.04
	2×4	$(0, 4) \rightarrow (1, 5) \rightarrow (2, 6) \rightarrow (3, 7)$	0.95	169 ms	10.4 cm	4.82	1.15
Temporal Coherence	1×4	$0 \rightarrow 1 \rightarrow 2 \rightarrow 3$	0.95	52.1 ms	4.3 cm	1.79	0.65
	1×4	Random	0.95	105 ms	8.2 cm	5.49	1.21
	1×4	$(0, 2) \rightarrow (1, 3)$	0.95	51.7 ms	6.8 cm	3.21	1.00
Confidence Level	1×4	$0 \rightarrow (1, 2) \rightarrow 3$	0.90	47.2 ms	7.9 cm	2.90	1.17
	1×4	$0 \rightarrow (1, 2) \rightarrow 3$	0.95	50.7 ms		3.12	1.28
	1×4	$0 \rightarrow (1, 2) \rightarrow 3$	0.99	155 ms		3.76	1.40

TABLE I: Performance of our planner in three different scenarios: *Different Arrangements*, *Temporal Coherence* and *Confidence Level*. We take into account different arrangement of blocks as well as the confidence levels used for probabilistic collision checking. These confidence levels are used for motion prediction. The prediction results in smoother trajectory and we observe up to 4X improvement in our smoothness metric defined in Equation (12). The overall planner runs in realtime.

Scenarios	Average Prediction Time	MHD	Smoothness	
			No Pred.	Pred.
Waving Arms	20.9 ms	5.0 cm	4.88	0.91
Moving Cans	51.7 ms	7.3 cm	5.13	1.04

TABLE II: Performance of the planner with a real robot running on the 7-DOF Fetch robot next to dynamic human obstacles. The planner runs in realtime and compute safe trajectories for challenging benchmark like "moving cans". We observe almost 5X improvement in the smoothness of the trajectory due to our prediction algorithm.

coherence, the human intention is predicted accurately with our approach with 100% certainty. In the random order, however, the human intention prediction step is not accurate until the human hand reaches the specific position. The personal order varies for each human, and reduces the possibility of predicting the next human action. When the right arm moves forward a little, $Fetch_0$ is predicted as the human intention with a high probability whereas $Fetch_1$ is predicted with low probability, even though position 1 is closer than position 0.

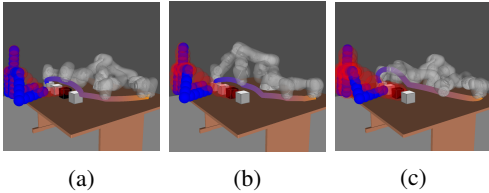


Fig. 5: **Probabilistic collision checking with different confidence levels:** A collision probability less $(1 - \delta_{CD})$ implies a safe trajectory. The current pose (i.e., blue spheres) and the predicted future pose (i.e. red spheres) are shown. The robot's trajectory avoids these collisions before the human performs its action. The higher the confidence level is, the longer the distance between the human arm and the robot trajectory. (a) $\delta_{CD} = 0.90$. (b) $\delta_{CD} = 0.95$. (c) $\delta_{CD} = 0.99$.

In the *Confidence Level* scenarios, we analyze the effect of confidence level δ_{CD} on the trajectory computed by the planner, the average task completion time, and the average motion planning time. As the confidence level becomes higher, the robot may not take the smoothest and shortest path so as to compute a collision-free path that is consistent with the confidence level.

In all cases, we observe the prediction results in smoother trajectory, using the smoothness metric defined as Equation (12). This is because the robot changes its path in advance

before the human obstacle actually blocks the robot's shortest path if human motion prediction is used.

B. Experiment with a Real Robot

We describe how our human motion prediction can help a robot avoid collisions with a human. In this experiment, a 7-DOF Fetch robot arm is used in the physical world. The robot delivers four soda cans from start locations to target locations on a desk. At the same time, the human sitting in front of the desk picks up and takes away the soda cans delivered to the target positions by the robot, which can cause collisions with the robot arm. In order to evaluate the collision avoidance capability of our approach, the human intentionally starts moving his arm to a soda can at a target location, blocking the robot's initially planned trajectory, when the robot is delivering another can moving fast. Our intention aware planner avoids collisions with the human arm and tends to compute a smooth trajectory.

Figure 1 shows two sequences of robot's trajectories. In the first row, the robot arm trajectory is generated an ITOMP re-planning algorithm without human motion prediction. As the human and the robot arm move too fast to re-plan collision-free trajectory. As a result, the robot makes collisions (the second figure) or very jerky trajectory (the third figure). In the second row, our human motion prediction approach is incorporated as described in Section V. The robot re-plans the arm trajectory before the human actually blocks its way, resulting in collision-free path.

VII. CONCLUSIONS AND FUTURE WORK

We present a novel intention-aware planning algorithm to compute safe robot trajectories in dynamic environments with human performing different actions. Our approach uses offline learning of human motions, decomposes different high-DOF human actions, and learns about their temporal

coherence in the given environment. At runtime, our approach uses the learned human actions to predict and estimate the future motions. We highlight the performance of our planning algorithm in complex benchmarks for human-robot cooperation in both simulated and real world scenarios with 7-DOF robots.

Our approach has some limitations. Our probabilistic collision checking formulation does not take into account robot control errors, which also affect to the collision probability. The performance of motion prediction algorithm depends on the variety and size of the learned data. Currently, we use supervised learning with labelled action types, but it will be useful to explore unsupervised learning based on appropriate action clustering algorithms.

REFERENCES

- [1] C. Plagemann, V. Ganapathi, D. Koller, and S. Thrun, "Real-time identification and localization of body parts from depth images," in *Robotics and Automation (ICRA), 2010 IEEE International Conference on*. IEEE, 2010, pp. 3108–3113.
- [2] J. Shotton, T. Sharp, A. Kipman, A. Fitzgibbon, M. Finocchio, A. Blake, M. Cook, and R. Moore, "Real-time human pose recognition in parts from single depth images," *Communications of the ACM*, vol. 56, no. 1, pp. 116–124, 2013.
- [3] R. Madhavan and C. I. Schlenoff, "Moving object prediction for off-road autonomous navigation," in *AeroSense 2003*. International Society for Optics and Photonics, 2003, pp. 134–145.
- [4] D. Vasquez, T. Fraichard, and C. Laugier, "Growing hidden markov models: An incremental tool for learning and predicting human and vehicle motion," *The International Journal of Robotics Research*, 2009.
- [5] T. Bandyopadhyay, C. Z. Jie, D. Hsu, M. H. Ang Jr, D. Rus, and E. Frazzoli, "Intention-aware pedestrian avoidance," in *Experimental Robotics*. Springer, 2013, pp. 963–977.
- [6] A. Turnwald, D. Althoff, D. Wollherr, and M. Buss, "Understanding human avoidance behavior: Interaction-aware decision making based on game theory," *International Journal of Social Robotics*, pp. 1–21, 2016.
- [7] V. V. Unhelkar, C. Pérez-Darpino, L. Stirling, and J. A. Shah, "Human-robot co-navigation using anticipatory indicators of human walking motion," in *Robotics and Automation (ICRA), 2015 IEEE International Conference on*. IEEE, 2015, pp. 6183–6190.
- [8] C. Fulgenzi, A. Spalanzani, and C. Laugier, "Dynamic obstacle avoidance in uncertain environment combining pvos and occupancy grid," in *Robotics and Automation, 2007 IEEE International Conference on*. IEEE, 2007, pp. 1610–1616.
- [9] J. van den Berg, S. Patil, J. Sewall, D. Manocha, and M. Lin, "Interactive navigation of multiple agents in crowded environments," in *Proceedings of the 2008 symposium on Interactive 3D graphics and games*. ACM, 2008, pp. 139–147.
- [10] S. Kim, S. J. Guy, W. Liu, D. Wilkie, R. W. Lau, M. C. Lin, and D. Manocha, "Brvo: Predicting pedestrian trajectories using velocity-space reasoning," *The International Journal of Robotics Research*, 2014.
- [11] P. Trautman, J. Ma, R. M. Murray, and A. Krause, "Robot navigation in dense human crowds: Statistical models and experimental studies of human-robot cooperation," *The International Journal of Robotics Research*, vol. 34, no. 3, pp. 335–356, 2015.
- [12] P. Turaga, R. Chellappa, V. S. Subrahmanian, and O. Udrea, "Machine recognition of human activities: A survey," *Circuits and Systems for Video Technology, IEEE Transactions on*, vol. 18, no. 11, pp. 1473–1488, 2008.
- [13] C. H. Ek, P. H. Torr, and N. D. Lawrence, "Gaussian process latent variable models for human pose estimation," in *Machine learning for multimodal interaction*. Springer, 2007, pp. 132–143.
- [14] R. Urtasun, D. J. Fleet, and P. Fua, "3d people tracking with gaussian process dynamical models," in *Computer Vision and Pattern Recognition, 2006 IEEE Computer Society Conference on*, vol. 1. IEEE, 2006, pp. 238–245.
- [15] K. Fragkiadaki, S. Levine, P. Felsen, and J. Malik, "Recurrent network models for human dynamics," in *Proceedings of the IEEE International Conference on Computer Vision*, 2015, pp. 4346–4354.
- [16] S. Nikolaidis, P. Lasota, G. Rossano, C. Martinez, T. Fuhlbrigge, and J. Shah, "Human-robot collaboration in manufacturing: Quantitative evaluation of predictable, convergent joint action," in *Robotics (ISR), 2013 44th International Symposium on*. IEEE, 2013, pp. 1–6.
- [17] K. P. Hawkins, N. Vo, S. Bansal, and A. F. Bobick, "Probabilistic human action prediction and wait-sensitive planning for responsive human-robot collaboration," in *Humanoid Robots (Humanoids), 2013 13th IEEE-RAS International Conference on*. IEEE, 2013, pp. 499–506.
- [18] H. S. Koppula and A. Saxena, "Anticipating human activities using object affordances for reactive robotic response," *Pattern Analysis and Machine Intelligence, IEEE Transactions on*, vol. 38, no. 1, pp. 14–29, 2016.
- [19] L. Busoniu, R. Babuska, and B. De Schutter, "A comprehensive survey of multiagent reinforcement learning," *Systems, Man, and Cybernetics, Part C: Applications and Reviews, IEEE Transactions on*, vol. 38, no. 2, pp. 156–172, 2008.
- [20] H. S. Koppula, A. Jain, and A. Saxena, "Anticipatory planning for human-robot teams," in *Experimental Robotics*. Springer, 2016, pp. 453–470.
- [21] E. A. Sisbot, L. F. Marin-Urias, R. Alami, and T. Simeon, "A human aware mobile robot motion planner," *Robotics, IEEE Transactions on*, vol. 23, no. 5, pp. 874–883, 2007.
- [22] A. D. Dragan, S. Bauman, J. Forlizzi, and S. S. Srinivasa, "Effects of robot motion on human-robot collaboration," in *Proceedings of the Tenth Annual ACM/IEEE International Conference on Human-Robot Interaction*. ACM, 2015, pp. 51–58.
- [23] D. Fox, W. Burgard, and S. Thrun, "The dynamic window approach to collision avoidance," *IEEE Robotics & Automation Magazine*, vol. 4, no. 1, pp. 23–33, 1997.
- [24] S. Petti and T. Fraichard, "Safe motion planning in dynamic environments," in *Proceedings of IEEE/RSJ International Conference on Intelligent Robots and Systems*, 2005, pp. 2210–2215.
- [25] C. Park, J. Pan, and D. Manocha, "ITOMP: Incremental trajectory optimization for real-time replanning in dynamic environments," in *Proceedings of International Conference on Automated Planning and Scheduling*, 2012.
- [26] J. Mainprice and D. Berenson, "Human-robot collaborative manipulation planning using early prediction of human motion," in *Intelligent Robots and Systems (IROS), 2013 IEEE/RSJ International Conference on*. IEEE, 2013, pp. 299–306.
- [27] R. S. Sutton and A. G. Barto, *Reinforcement learning: An introduction*. MIT press, 1998.
- [28] M. Müller, "Dynamic time warping," *Information retrieval for music and motion*, pp. 69–84, 2007.
- [29] E. Snelson and Z. Ghahramani, "Sparse gaussian processes using pseudo-inputs," in *Advances in neural information processing systems*, 2005, pp. 1257–1264.
- [30] N. E. Du Toit and J. W. Burdick, "Probabilistic collision checking with chance constraints," *Robotics, IEEE Transactions on*, vol. 27, no. 4, pp. 809–815, 2011.
- [31] *Prime Sensor NITE 1.3 Algorithms notes*, PrimeSense Inc., 2010, last viewed 19-01-2011 15:34. [Online]. Available: <http://www.primesense.com>
- [32] J. Zhu and T. Hastie, "Kernel logistic regression and the import vector machine," *Journal of Computational and Graphical Statistics*, 2012.
- [33] C. W. Groetsch, "The theory of tikhonov regularization for fredholm equations of the first kind," 1984.
- [34] M. Quigley, K. Conley, B. Gerkey, J. Faust, T. Foote, J. Leibs, R. Wheeler, and A. Y. Ng, "Ros: an open-source robot operating system," in *ICRA workshop on open source software*, vol. 3, no. 3.2. Kobe, Japan, 2009, p. 5.
- [35] M.-P. Dubuisson and A. K. Jain, "A modified hausdorff distance for object matching," in *Pattern Recognition, 1994. Vol. 1-Conference A: Computer Vision & Image Processing, Proceedings of the 12th IAPR International Conference on*, vol. 1. IEEE, 1994, pp. 566–568.